Original Article
Yonsei Med J 2016 Jul;57(4):1006-1015
http://dx.doi.org/10.3349/ymj.2016.57.4.1006
Yonsei Medical Journal
YMJ
pISSN: 0513-5796 · eISSN: 1976-2437

Preclinical Study of Cell Therapy for Osteonecrosis of the Femoral Head with Allogenic Peripheral Blood-Derived Mesenchymal Stem Cells

Qiang Fu[1], Ning-Ning Tang[1], Qian Zhang[2], Yi Liu[3], Jia-Chen Peng[3], Ning Fang[1], Li-Mei Yu[1], Jin-Wei Liu[1], and Tao Zhang[1]

[1]Key Laboratory of Cell Engineering of Guizhou Province, The Affiliated Hospital of Zunyi Medical College, Zunyi, Guizhou;
[2]Department of Human Anatomy, Zunyi Medical College, Zunyi, Guizhou;
[3]Department of Bone and Joint Surgery, The Affiliated Hospital of Zunyi Medical College, Zunyi, Guizhou, China.

Purpose: To explore the value of transplanting peripheral blood-derived mesenchymal stem cells from allogenic rabbits (rPBMSCs) to treat osteonecrosis of the femoral head (ONFH).

Materials and Methods: rPBMSCs were separated/cultured from peripheral blood after granulocyte colony-stimulating factor mobilization. Afterwards, mobilized rPBMSCs from a second passage labeled with PKH26 were transplanted into rabbit ONFH models, which were established by liquid nitrogen freezing, to observe the effect of rPBMSCs on ONFH repair. Then, the mRNA expressions of BMP-2 and PPAR-γ in the femoral head were assessed by RT-PCR.

Results: After mobilization, the cultured rPBMSCs expressed mesenchymal markers of CD90, CD44, CD29, and CD105, but failed to express CD45, CD14, and CD34. The colony forming efficiency of mobilized rPBMSCs ranged from 2.8 to 10.8 per million peripheral mononuclear cells. After local transplantation, survival of the engrafted cells reached at least 8 weeks. Therein, BMP-2 was up-regulated, while PPAR-γ mRNA was down-regulated. Additionally, bone density and bone trabeculae tended to increase gradually.

Conclusion: We confirmed that local transplantation of rPBMSCs benefits ONFH treatment and that the beneficial effects are related to the up-regulation of BMP-2 expression and the down-regulation of PPAR-γ expression.

Key Words: Osteonecrosis of the femoral head (ONFH), peripheral blood, mesenchymal stem cells (MSCs), cell transplantation, disease model, rabbit

INTRODUCTION

Osteonecrosis of the femoral head (ONFH) results from the disruption of blood supply to the femoral head (FH), gradually leading to the necrosis of osteocytes and marrow and eventually resulting in osteoarthritis and osteonecrosis.[1-4] However, as the condition is still somewhat rare, effective treatments are lacking. Although traditional therapies, such as medication and surgery, are beneficial in the early stages of ONFH, its natural progression gradually leads to a wider osteonecrosis and ultimately results in the collapse of FH. Eventually, a total hip replacement has to be performed.[5-7] Therefore, novel and effective therapies against ONFH are urgently needed.

Studies on stem cell therapy have focused on ONFH.[8,9] Among somatic stem cells, bone marrow-derived mesenchymal stem cells (BMMSCs) are considered a primary source, because they can be obtained relatively easily. Adipose-derived mesenchymal stem cells (ADSCs) are another source of stem cells, and are present in larger numbers than BMMSCs.[10] The effects of

Received: October 23, 2015 **Revised:** November 23, 2015
Accepted: December 9, 2015
Corresponding author: Dr. Tao Zhang, Key Laboratory of Cell Engineering of Guizhou Province, The Affiliated Hospital of Zunyi Medical College, No.149 Dalian Rd., Huichuan District, Zunyi 563000, Guizhou, China.
Tel: 86-851-28608806, Fax: 86-851-28622043, E-mail: oceanzt@163.com

•The authors have no financial conflicts of interest.

both cell therapies have yielded satisfactory results.[11-15] However, bone marrow collection is restricted by the patient's condition and age,[13] and the invasive procedure may result in infection. As for ADSCs, a standardization process is still absent. Therefore, to explore substitute resources from which mesenchymal stem cells (MSCs) can be more conveniently obtained has emerged as a new focus. The existence of peripheral blood-derived mesenchymal stem cells (PBMSCs) has been confirmed by some recent research.[16-18] As harvesting blood is a less invasive and cheaper way to obtain stem cells, it could offer significant advantages for autologous use. Indeed, there have been a few reports about treatment with PBMSC transplantation (PBMSCT) on tissue damaged diseases. According to a previous study, we found that there was a significant increase in the number of PBMSCs observed after recombinant human granulocyte colony-stimulating factor (G-CSF) mobilization.[19] In this study, rabbit PBMSCs (rPBMSCs) were enriched after G-CSF mobilization. The enriched PBMSCs were implanted in the necrotic areas of ONFH, and the results revealed that the therapeutic efficiency by PBMSCT after core compression (CD) is superior to that by simplex CD. In addition, this present study suggests that this beneficial effect relates to the up-regulation of BMP-2 expression and down-regulation of PPAR-γ expression after PBMSCT, which lays the foundation for further exploration of the molecular mechanism of ONFH treatment by PBMSCT.

MATERIALS AND METHODS

Isolation and culture of mobilized rPBMSCs

New Zealand rabbits (n=36), which were purchased from Chongqing Xin Teng Biological Technology Co., Ltd. (production license: SCXK Yu 2012–0005), were selected regardless of sex. The committee for experimental animals of Zunyi Medical College approved all of the experimental procedures, and the procedures complied with the Guidelines for the Care and Use of Laboratory Animals. The three-month old rabbits were selected and underwent a continuous subcutaneous injection of G-CSF for mobilization according to the dose of 30 μg/kg/d for 6 days. Afterwards 20 mL of peripheral blood (PB) were collected with sodium heparin, diluted in 20 mL of phosphate buffer saline (PBS) and layered over the 20 mL of Ficoll (1.073 g/L, Virtue Pacific, Tianjin, China). After density gradient centrifugation (Centrifuge 5804R, Eppendorf, Germany) at 2000 rpm for 25 min, the buffy coat layer rich in mononuclear cells was harvested and washed twice with PBS. Thereafter, the erythrocytes were lysed by red blood cell lysis solution. Subsequently, the collected cells were rinsed twice, and the supernatant was removed. Then, the cells were re-suspended, counted, and plated at $5\times10^5/cm^2$ in a T25 disposable plastic flask at 37°C, in a humidified 5% CO_2 incubator (Forma 3141, I/R, Thermo, Waltham, MA, USA), in 5 mL of low glucose-Dulbecco's modified eagle medium (LG-DMEM, Gibco, New York, NY, USA) supplemented with 15% fetal bovine serum (FBS, Gibco, New York, NY, USA), 100 U/mL penicillin, 100 μg/mL streptomycin, and 2 mmol/L L-glutamine (Glu, HyClone, Logan, UT, USA). The growth status of those cells was observed after approximately 24 h under a light microscope (YS100, Nikon, Tokyo, Japan). Half of the medium was replaced after 72 h, and the full medium was replaced every 2 days until the cell growth reached approximately 80–90% confluence. Finally, the cells were seeded at a density of $2–5\times10^5$/mL for subculture.

Phenotypic identification of mobilized rPBMSCs

Flow cytometry analysis

Passage 2 rPBMSCs were digested with 0.125% trypsin-0.02% ethylenediamine tetraacetic acid disodium salt (EDTA-2Na, Calbioche, Darmstadt, Germany) and suspended. After density gradient centrifugation at 1500 rpm for 5 min, the cell supernatant was removed and the cell concentration was adjusted to 2×10^6/mL by adding appropriate Dulbecco's Phosphate Buffered Saline (D-PBS). The liquid was placed into flow tubes, 100 μL per tube, and then anti-rabbit CD29-FITC (Millipore, Billerica, MA, USA) and CD14-PE (Acris Antibodies, San Diego, CA, USA) were added to the tubes, respectively, for labeling of the cells. After incubation for 20 min away from light, 2 mL of D-PBS containing 0.1% NaN_3 was added to mix and shaken. After centrifugation, as stated above, the supernatant was removed, and 200 μL of 1% paraformaldehyde fixative solution (PFA) was added and oscillated until uniform. Then, the cells were preserved at 4°C until ready for flow cytometry analysis (FACS Calibur, Becton Dickinson, Franklin Lakes, NJ, USA) within 24 h using Cell Quest software. The number of collected cells was not less than 2×10^4, and the isotype control antibodies were IgG-FITC (Millipore, Billerica, MA, USA) and IgG2a-PE (Millipore, Billerica, MA, USA) of mouse derivation.

Immunocytochemical staining analysis

After preparation of climbing slices of passage 2 rPBMSCs, the cells were washed 3 times with PBS for 5 min. Those cells were fixed in 4% PFA for 15 min at room temperature, and then they were washed with PBS again as stated above. Afterwards, goat serum (Boster, Wuhan, China) was added dropwise, incubated for 30 min at room temperature, and then shaken to dry. Thereafter, primary antibodies, including anti-rabbit CD90 (Millipore, Billerica, MA, USA), CD105, CD34 (Biorbyt, Shanghai, China), CD45, and CD44 (AbD serotec, Oxford, UK), were added to rPBMSCs, respectively, according to the manufactures' instructions, and then incubated overnight at 4°C. Meanwhile, PBS was used as a substitute for primary antibodies as a control. Then, the secondary antibodies against rabbits were added to rPBMSCs according to the instructions provided in the immunohistochemistry kit, and incubated for 30 min at 37°C. rPBMSCs were rinsed with PBS again, as stated above, subse-

quently stained with Diaminobenzidine (Gene Tech, Shanghai, China) for 5 min, and washed with tap water. Finally, after counterstaining with hematoxylin for 30 s, rPBMSCs were washed with tap water again and observed under the inverted microscope (IX-71-S8F, Olympus, Tokyo, Japan) after air drying.

Colony-forming ability and other characteristics of mobilized rPBMSCs

The colony forming efficiency (CFE) of rPBMSCs was analyzed according to a previous report.[19] Briefly, mononuclear cells of mobilized rabbit PB samples and non-mobilized ones were counted and seeded at $5\times10^5/cm^2$ into six-well plates, respectively. The cells were cultured at 37°C in a humidified 5% CO_2 atmosphere with α-MEM (Gibco, New York, NY, USA) supplemented with 15% FBS, 100 U/mL penicillin, and 100 μg/mL streptomycin. Half of the culture medium was replaced 3 days later, and the full medium was replaced 5 days later, after which full medium was replaced every 3 days. After 14 days, the cells were fixed in 4% PFA, and stained for 5 min with crystal violet, and colony forming units (CFU) for which cell numbers were greater than 50 were counted under an anatomical lens. CFE= number of CFU/number of inoculated mononuclear cells (/10^6 as unit). Mesoderm multi-lineage differentiation capacities were analyzed according to our previous research.[16]

Establishment of a rabbit ONFH model and mobilized rPBMSCs implantation

A rabbit ONFH model was established by a liquid nitrogen freezing method (Fig. 1A-D) according to our previous report.[20] Bilateral FHs were both established as ONFH models, the right for implantation and the left for validation of the approach. Then, the rabbits were randomly divided into four groups: control group, model group, CD group, and PBMSCT group. After the establishment of ONFH models, all animal models in the CD and PBMSCT groups underwent core decompression of the FHs. Briefly, a drill, the diameter being 1.2 mm, was inserted to a 5-mm depth, at an angel of 45° from the posteromedial femoral neck (Fig. 1G), until the drill arrived at the underside of articular cartilage (Fig. 1E). As for the PBMSCT group, mobilized rPBMSCs of passage 2 or passage 3 were injected at 3×10^6 cells per model after CD. Later, the wounds of all rabbits were closed layer by layer (Fig. 1F), and penicillin was administered for preventing infection via an intramuscular injection at 4×10^5 U/d for 5 days.

Tracing the survival of mobilized rPBMSCs after implantation

Passage 2 rPBMSCs were marked with PKH26 Red Fluorescent Cell Linker (Sigma, St. Louis, MO, USA) according to the instructions of the manufacturer, and then transplanted into

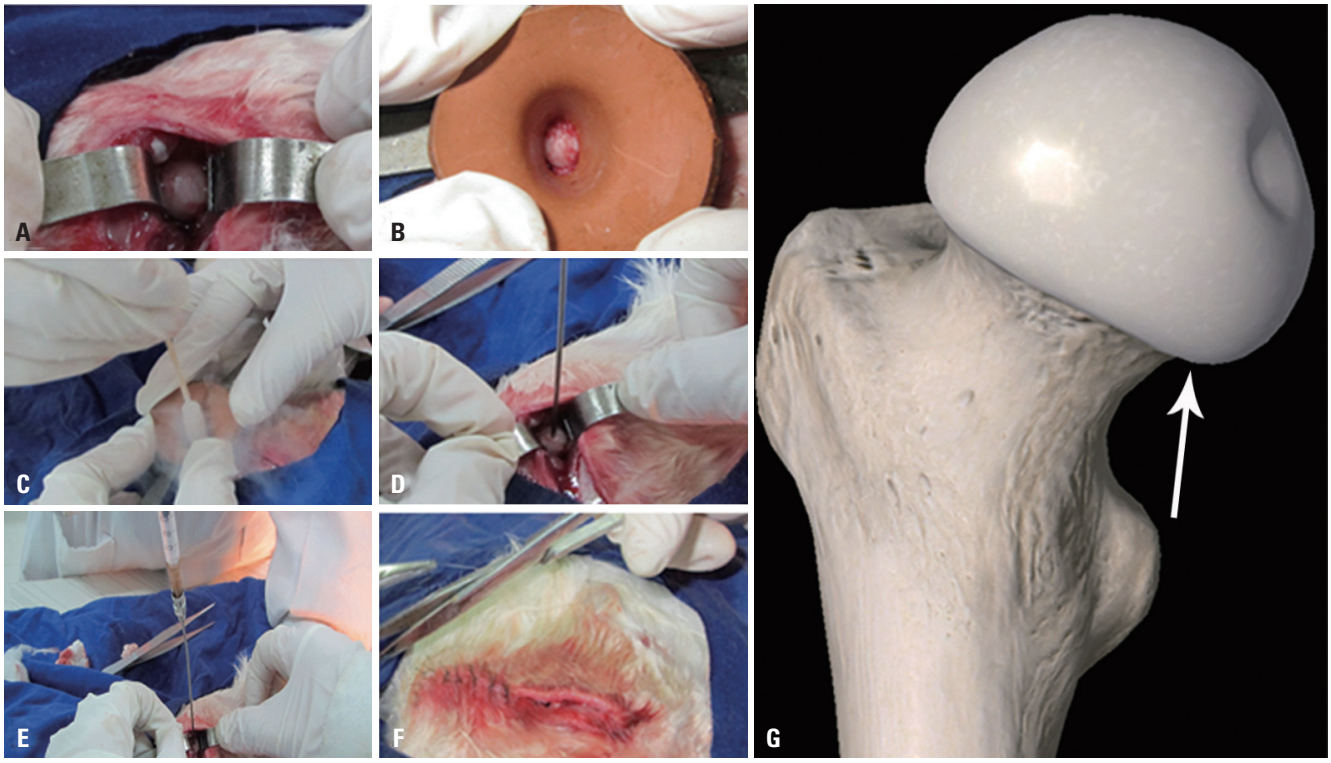

Fig. 1. Operation process of the establishment of rabbit model by liquid nitrogen freezing. (A) Blunt separation of the gluteus maximus muscle, gluteus medius muscle, and gluteus minimus muscle. (B) Dislocation of femoral head and covering it with a rubber funnel. (C) Freezing the femoral head with liquid nitrogen by medical cotton stickers. (D) Drilling a 5 mm-depth hole at an angle of 45° from the posteromedial femoral neck according to the direction of the arrow until the bit arrived at the underside of articular cartilage. (E) Injection of PBMSCs of passage 2 or passage 3 after drilling. (F) Suture of the wound layer by layer. (G) Direction of the drilling. PBMSCs, peripheral blood-derived mesenchymal stem cells.

http://dx.doi.org/10.3349/ymj.2016.57.4.1006

the FH through the bone tunnel. Thereafter, FHs from three of the models were removed at 2 weeks, 6 weeks, and 8 weeks, respectively. After being fixed in 4% PFA for 48 h, the fresh FH tissue specimens underwent decalcification, the decalcifying fluid being 1 mol/L EDTA, at 37°C in a Shaking Bath (SBD 50, Heto-Holten, Waltham, MA, USA) for 14 days. Afterward, longitudinal sections, the thickness being 15 μm, were made by freezing microtomes (CM1850, Leica, Solms, Germany). After counterstaining with DAPI Fluorescent Cell Linker (Sigma, St. Louis, MO, USA), the survival of transplanted rPBMSCs were observed under a fluorescence microscope (DMIR, Leica, Solms, Germany).

Radiographs of hip joints

Rabbits were injected with 3% carbrital at 30 mg/kg through the auricular vein, and then fixed on a checking platform at the dorsal decubitus. Positive photographs of bilateral hip joints were taken by X-ray machine (AXIOM Aristos VX, Siemens, Berlin, Germany), and the imaging features, including shape of FHs, bone densities, and joint spaces, in each group were observed.

Histopathology analysis of FH

After fixed in 4% PFA for 48 h, the fresh FH specimens were decalcified with 20% formic decalcified fluid (pH=6.0) supplemented with 20 mL of formic acid and 80 mL of formalin for 3 weeks. Subsequently, the specimens were embedded in paraffin and sectioned at 5-μm thickness by a paraffin-splicing machine (RM2235, Leica, Solms, Germany). Thereafter, three fields of each section were randomly selected to observe the histopathologic characteristics under a light microscope after hematoxylin and eosin (HE) staining.

Detection of the mRNA expressions of BMP-2 and PPAR-γ in local tissue from FHs

Primer sequences were designed by Primer Premier 6 and synthesized by Shanghai Generay Biotech Co., Ltd. The forward primer sequence of BMP-2 was 5′-TCGAGAACAGATG CAGGAAG-3′, and the reverse one was 5′-GGAATTTCGAGT TGGCTGTT-3′. The forward primer sequence of PPAR-γ was 5′-GCAAAGAAGTCGCCATCC-3′, and the reserve one was 5′-GGGCTCCATAAAGTCACCAA-3′. The forward primer sequence of β-actin gene, as an internal control, was 5′-AGGC CAACCGCGAGAA-3′, and the reserve one was 5′-CCGTCGCC AGAGTCCAT-3′.

Fresh specimens of FH tissues (n=24) were collected from 3 animals at 2 weeks and 8 weeks, respectively. Total intracellular RNA was extracted according to the instructions provided by RNAiso™ Plus (TaKaRa, Dalian, China), and then, a reverse transcription reaction was performed by a PrimeScript® RT Reagent Kit (TaKaRa, Dalian, China). The reaction volume was 20 μL; the total RNA was 100 ng; and the reaction conditions was set to 37°C for 15 min and then 85°C for 5 s. The reaction system of fluorescent quantitative PCR was carried out with a SYBR® Premix Ex Taq™ II Kit (TaKaRa, Dalian, China) in a 25-μL reaction volume supplemented with 12.5 μL of SYBR® Premix Ex Taq™ II (2×), 1 μL of upstream primers and 1 μL of downstream ones (10 μmol · L^{-1}), 1 μL of template cDNA

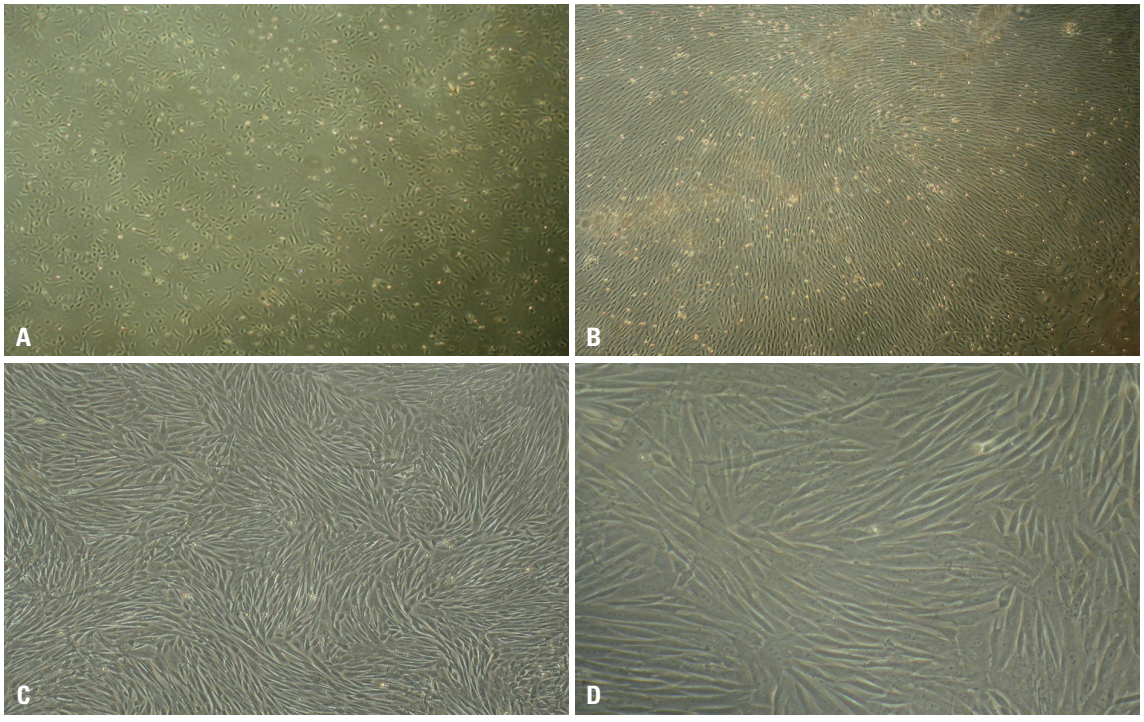

Fig. 2. Morphology of cultured rPBMSCs. (A) Primary colony growth of rPBMSCs for 3 d ×40. (B) Primary confluent growth of rPBMSCs for 10 d ×100. (C) The second passage of rPBMSCs ×200. (D) The second passage of rPBMSCs ×200. rPBMSCs, peripheral blood-derived mesenchymal stem cells from rabbits.

(equivalent to 5 ng total RNA), and 9.5 μL of RNase Free dH_2O. The reaction conditions were set to 95°C for 30 s for initial denaturation, then 95°C for 5 s, and 60°C for 30 s until the operation cycled 40 times. Finally, the specificity of the PCR products was identified by agarose gel electrophoresis (Syngene, Cambridge, UK), and a relative quantitative analysis was performed according to the method previously reported.[21]

Statistical analyses

Data are presented as mean±standard error (SEM). Statistical analyses were performed using the SPSS 13.0 software package (SPSS Inc., Chicago, IL, USA), and one-way ANOVA was conducted for comparisons between groups. Statistical significance was set at $p<0.05$.

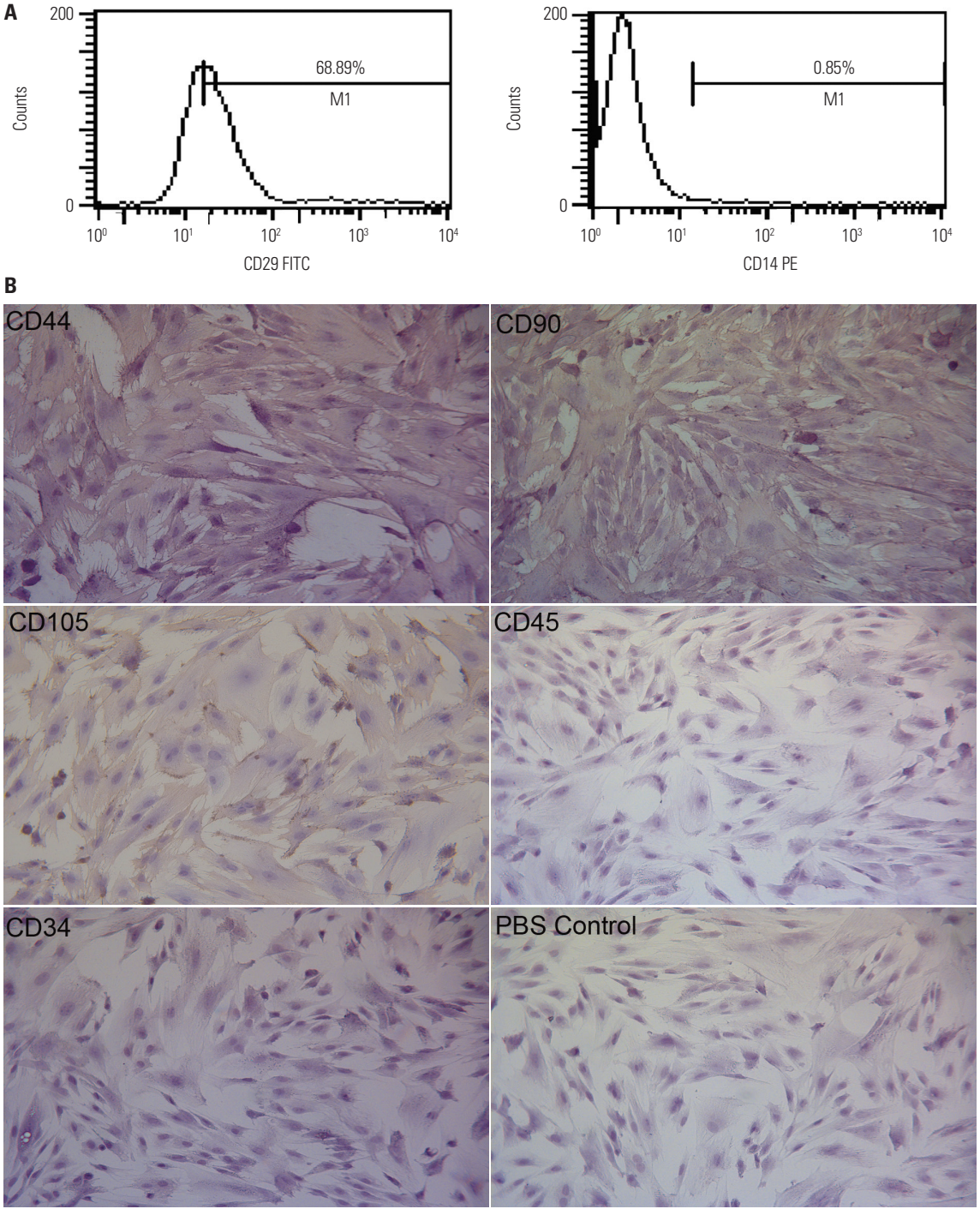

Fig. 3. Phenotypic analysis of mobilized rPBMSCs. (A) Demonstration of the positive expression of CD29 and the negative expression of CD14 by FCM. (B) Positive expression of CD44, CD105, and CD90, and negative expression of CD45 and CD34 by immunocytochemical staining ×200. rPBMSCs, peripheral blood-derived mesenchymal stem cells from rabbits; FCM, flow cytometer; PBS, phosphate buffer saline.

http://dx.doi.org/10.3349/ymj.2016.57.4.1006

RESULTS

Mobilized rPBMSCs owned the growth characteristics of MSCs

Spindle adherent cells were observed after 24 h of primary culture of mobilized rabbit peripheral blood mononuclear cells (PBMNCs). The colonies of adherent cells formed obviously after 72 h of primary culture (Fig. 2A), and those cells could grow to 80% approximately confluence after 10 days of primary culture (Fig. 2B). The passage cells possessed uniform long-shuttle-like morphology and showed a whirl-like arrangement growth (Fig. 2C and D). As for the non-mobilized PB samples, there were few adherent cells observed after the 24-hour primary culture, and few cell colonies formed 10 days after primary culture. Subsequently, the cultured cells aged quickly and failed to subculture.

Mobilized rPBMSCs owned the phenotypic analysis of MSCs

The flow cytometry results of mobilized rPBMSCs from passage 2 indicated the positive expression of CD29 and negative expression of CD14 (Fig. 3A). The immunocytochemical staining results indicated positive expression of CD44, CD105, and CD90 and negative expression of CD45 and CD34 (Fig. 3B).

Mobilized rPBMSCs owned a higher CFE and differentiation capacities of MSCs

The colony-forming test showed that colonies could be successfully obtained from all of the collected mobilized PB samples, while only one out of the four non-mobilized samples produced a few colonies. The CFE was 2.8–10.8/10^6 from mobilized PB (Fig. 4A and B) and 0–3/10^6 from non-mobilized PB (Fig. 4C and D). That is, there was 6.76±2.42 PBMSCs per million PBMNCs after mobilization, outnumbering 0.75±1.29 in the non-mobilized group (p<0.01) (Fig. 4E). rPBMSCs could differentiate into osteocytes (Fig. 4F), adipocytes (Fig. 4G), and chondrocytes (Fig. 4H).

PKH26-marked mobilized rPBMSCs could survive at least 8 weeks *in vivo*

rPBMSCs could be successfully marked with PKH-26 *in vitro* (Fig. 5A and B). Observation results of FH tissue slices suggested that rPBMSCs marked with PKH26 could be found in the necrotic area up to 8 weeks after transplantation, although the number of the engrafting cells in the necrotic zone significantly decreased as time elapsed (Fig. 5C).

PBMSCT enhanced the bone regeneration *in vivo*

At 8 weeks, there was an obvious collapse, lessened shape, serious defect, greater joint space, and even a joint abnormal alignment, and the epiphyseal plate became indistinct in the model group (Fig. 6A). That is, the overall shape of FHs showed an aggravated development with loss of time. Meanwhile, the

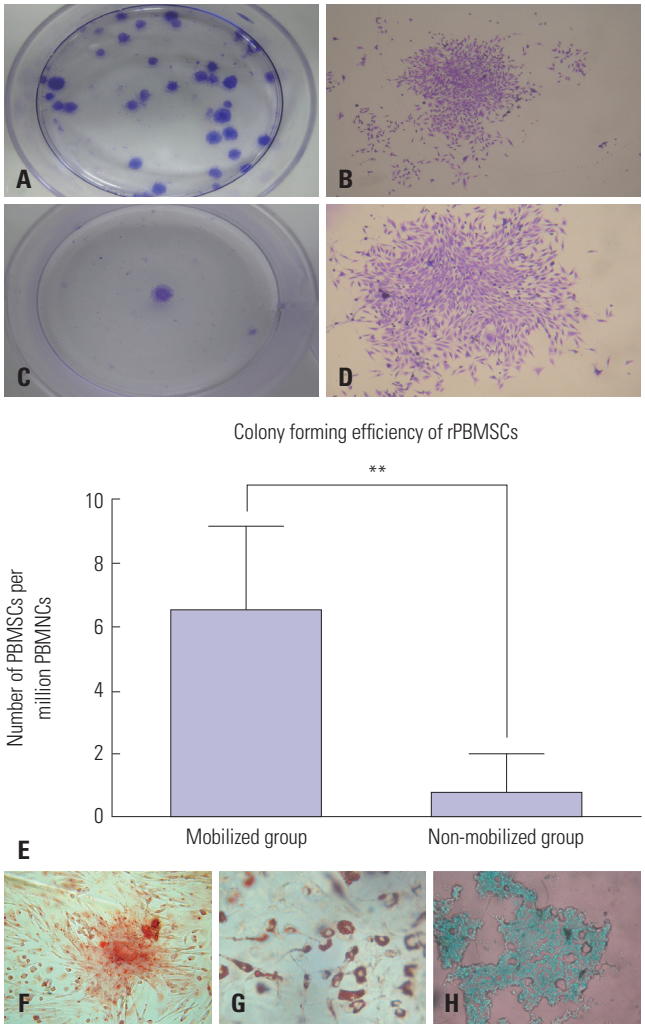

Fig. 4. CFE and differentiation capacities of cultured rPBMSCs. (A) Colony-forming ability of CFU-F isolated from mobilized rabbit peripheral blood. (B) One CFU-F of mobilized peripheral blood under a light microscope. (C) Colony-forming ability of CFU-F isolated from non-mobilized rabbit peripheral blood. (D) CFU-F of non-mobilized peripheral blood under a light microscope. (E) Comparison of CEF between mobilized peripheral blood and non-mobilized one. (F) Osteogenesis-committed differentiation of PBMSCs by alizarin red ×400. (G) Adipogenesis-committed differentiation of PBMSCs stained by oil red O ×400. (H) Chondrogenesis-committed differentiation of PBMSCs stained by alcian blue ×400. **p<0.01. CFE, colony forming efficiency; rPBMSCs, peripheral blood-derived mesenchymal stem cells from rabbits; CFU, colony forming units; PBMNCs, peripheral blood mononuclear cells.

density of all FHs in the CD group increased continually, and the central zone was lower, and the edge was higher. Additionally, sclerosis lines appeared (Fig. 6B). In the PBMSCT group, beside the representation of high-density image of FH, trabecular bone appeared intact and well-distributed (Fig. 6C). The whole densities in the PBMSCT group were higher than those in the simplex CD group.

PBMSCT increased bone regeneration and decreased pimelosis

At 8 weeks, the adipose cells in the medullary cavity hypertro-

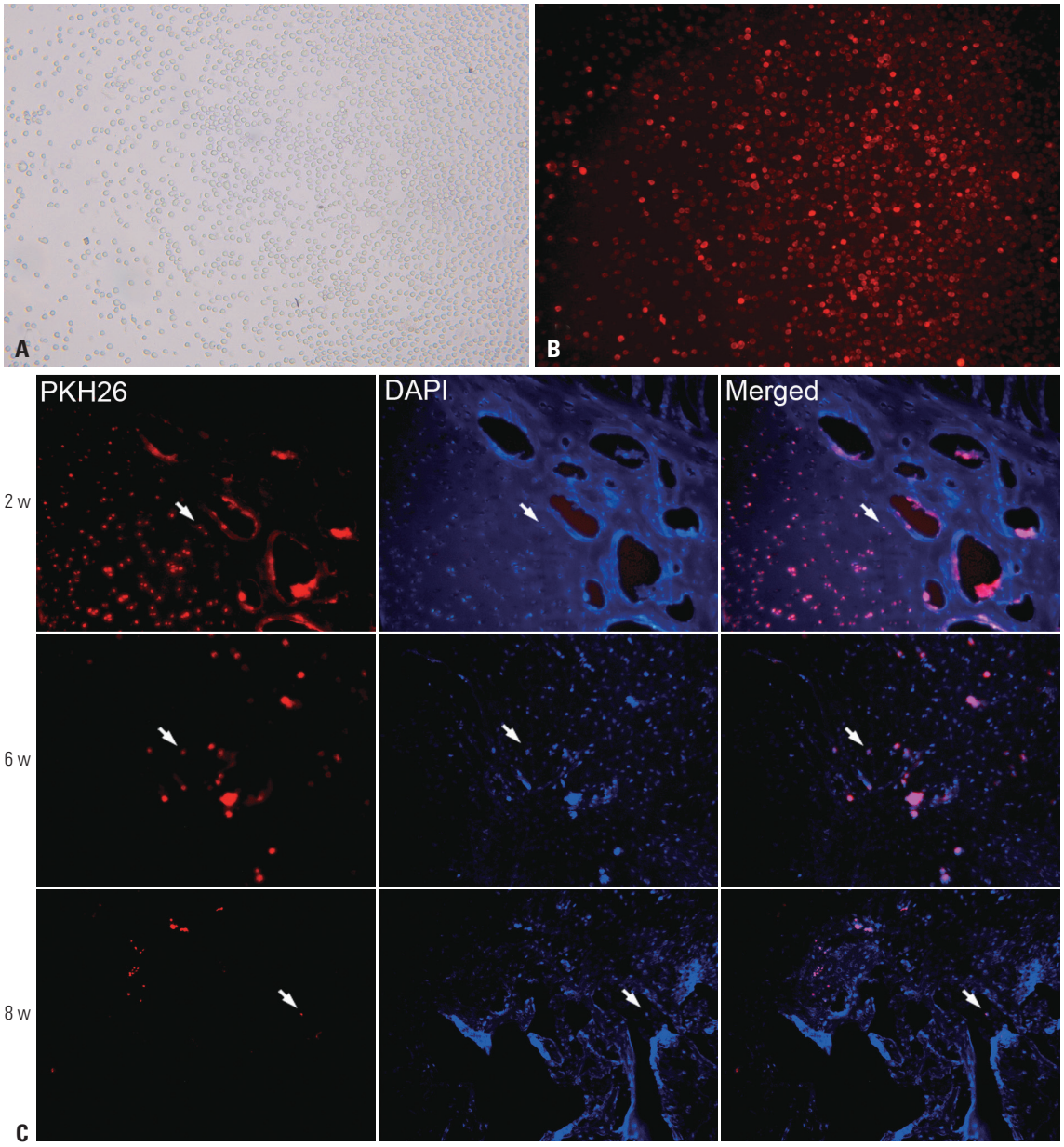

Fig. 5. Labelling *in vitro* and survival *in vivo* of mobilized rPBMSCs after implantation. (A) View of PKH26-labelled PBMSCs *in vitro* under phase contrast microscope ×100. (B) View of PKH26-labelled PBMSCs *in vitro* under a fluorescent microscope ×100. (C) rPBMSCs marked with PKH26 and DAPI could be found in the lesion site at 2 weeks, less conspicuously at 6 weeks, and faintly at 8 weeks as the arrow pointed ×100. rPBMSCs, peripheral blood-derived mesenchymal stem cells from rabbits.

phied, some of which even fused into vesicles and hematopoietic tissues obviously decreased. Bone chips, disorders, and faults in trabecular bone, as well as empty lacunae of osteocytes and the extrusion deformation of cells, were widely observed in the model group. The percentage of the bone trabecular area was 29.66%, lower than that in the control group, which was 54.82% (p<0.01) (Fig. 6D and G). In the CD group, the repair still existed around the drilled holes. Bone marrow and the non-uniform distribution of trabecular bone could be observed, and the percentage the bone trabecular area was 49.01%, higher than the model group (p<0.05) (Fig. 6E and G). While in the PBMSCT group, the trabecular bone tended to be matured and a large amount of bone marrow existed in the drilled holes. The percentage was 57.32%, higher than the model group (p<0.05) (Fig. 6F and G).

Up-regulation of BMP-2 expression and down-regulation of PPAR-γ expression after PBMSCT

The mRNA expression of BMP-2 in the PBMSCT group, presenting a gradual uptrend, was obviously higher than that in the corresponding CD group at each time point, and the difference was significant at 2 weeks (p<0.05) and 8 weeks (p<0.01), although lower than the normal group (Fig. 6H and J). As for PPAR-γ mRNA, expression was always higher than the normal

http://dx.doi.org/10.3349/ymj.2016.57.4.1006

in the PBMSCT and CD groups. Compared with the CD group, the mRNA expression of PPAR-γ after PBMSCT initially had no significance at 2 weeks (Fig. 6I); however, there were significant differences at 8 weeks (p<0.01) (Fig. 6K).

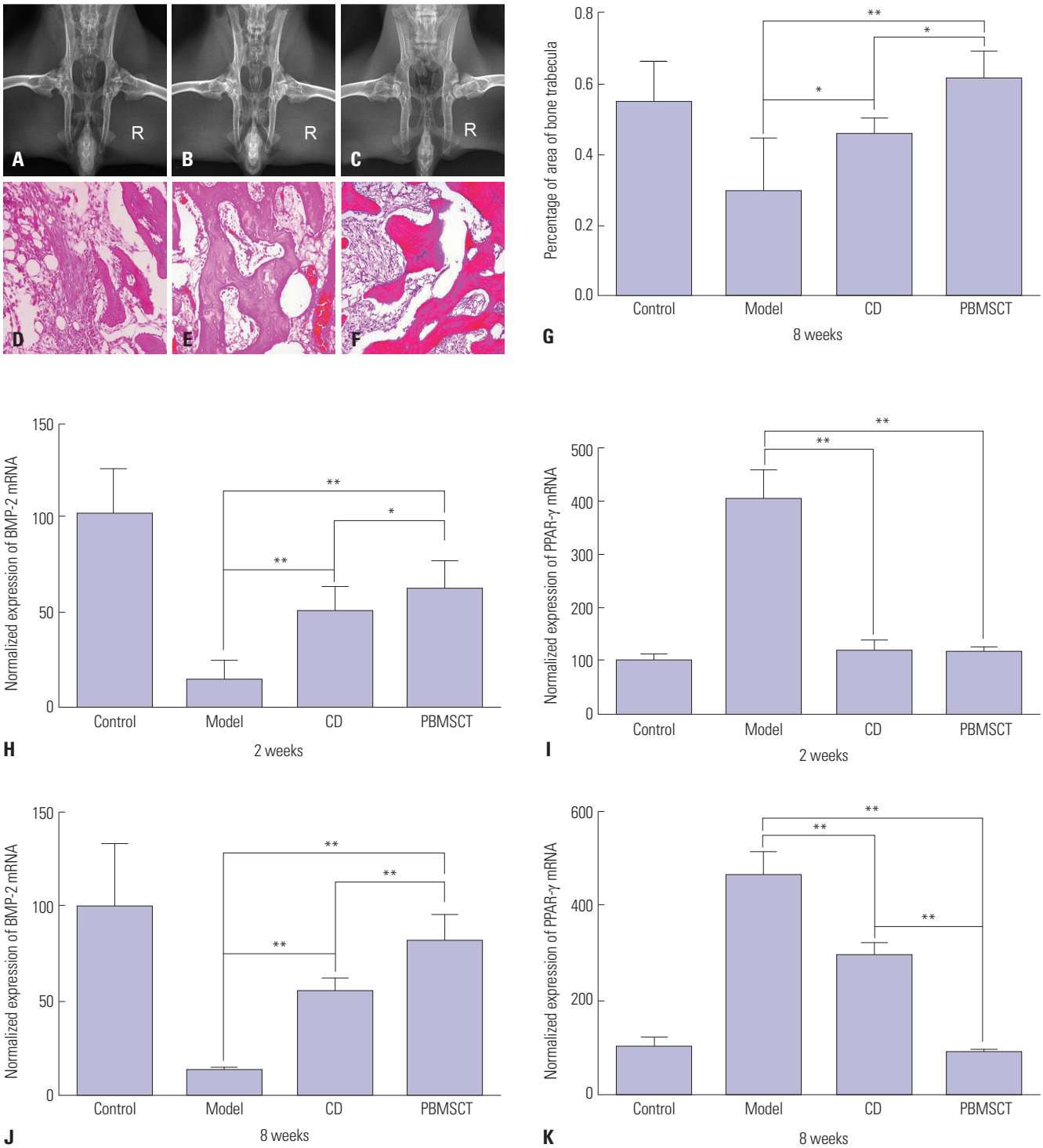

Fig. 6. Radiographs, histopathologic changes, and expression of BMP-2 and PPAR-γ of FHs in all rabbit groups. (A) There were obvious collapse, lessened shape, serious defect, greater joint space, and even a changed para position in the control group. (B) The central zone density was lower, while the edge higher and the sclerosis lines appeared in the CD group. (C) High-density image and bone trabeculae appeared in the PBMSCT group at 8 w. (D) Post-operation HE staining of the model group, (E) CD group, and (F) PBMSCT group at 8 w ×100. (G) Percentage of area of bone trabeculae. (H) Expression of BMP-2 at 2 weeks. (I) Expression of PPAR-γ at 2 weeks. (J) Expression of BMP-2 at 8 weeks. (K) Expression of PPAR-γ at 8 weeks. *p<0.05, **p<0.01. FH, femoral head; CD, core decompression; HE, hematoxylin and eosin; PBMSCT, peripheral blood-derived mesenchymal stem cells transplantation.

DISCUSSION

Analysis of CFE of PBMNCs, according to the adherent culture method,[22] indicated that the frequency of adult human PBMSCs ranged from 0.5 to 5 per million mononuclear cells, which is 1/20 to 1/5 of human BMMSCs. This research found that the frequency of rPBMSCs ranged from 2.8 to 10.8 per million mononuclear cells, which was in line with the previous report and at the same order of magnitude with human PBMSCs.[23] In order to meet the transplantation demand of cell amount, the donor cells needed isolation and amplification culture *in vitro*. Given that there was a lesser amount of PBMSCs than BMMSCs, the experimental animals were mobilized with G-CSF. As expected, we could get about 9-fold cells after G-CSF than that without mobilization. Phenotype analysis of rPBMSCs in this study demonstrated that the cells simultaneously expressed CD29, CD44, CD90, and CD105, but failed to express CD34, CD45, and CD14, consistent with the phenotypic characteristics of MSCs.[24,25] That is, the isolated and cultured cells in the present study were highly purified PBMSCs. Additionally, the amount of passage 2 mobilized PBMSCs from each rabbit reached 6–8×10^6, which could meet the PBMSCT demands for two rabbit ONFH models.

In terms of experimental animals, rabbits were selected as the object of this study in consideration of the effective cost, easy operation, and coincident physiology with humans.[26] In this research, the greater trochanter of the femur was chosen as the cut mark, and thus reduced unnecessary injury. Blunt dissection of muscle decreased bleeding. Frozen necrosis was administered through the dipping of liquid nitrogen with medical cotton stickers, which provided better control of the intensity of frozen necrosis than noted in a previous study.[20,27,28] Results of radiograph and histopathological morphology analysis suggested that the pathological change of rabbit ONFH models represented an aggravating trend and ultimately resulted in the collapse and dysfunction of hip joints.

Although there have been many experimental and clinical application studies on the treatment of ONFH with BMMSCs[12,29-33] and the effect is convincing, the experimental evidence of internal survival and the function in tissue repair of BMMSCs has always been unclear. It is inferred that the therapeutic effect of BMMSCs relates to how it could participate in the repair process and secrete some cellular factors, which are beneficial to bone regeneration. In addition, autogenous immunocytes can also be advantageous to BMMSCs.[18] In this paper, PBMSCs marked with PKH26 could be found in the necrotic area 8 weeks after transplantation. However, the numbers of engrafting cells decreased as time passed, proving that the survival of those grafted cells arrived at no less than 8 weeks. As for the whereabouts of the decreased cells, whether they differentiate into other cells or are apoptotic, remains unclear. Results of radiograph and histopathological morphology analysis showed that there were more neonatal bone trabeculae and bone marrow appeared in the PBMSCT group, which indicated that the treatment effect after PBMSCT is superior to CD.

Until now, the mechanism of the treatment of tissue injury diseases by PBMSCs, just as by BMMSCs, is ill-defined. In this research, the mRNA expressions of BMP-2 and PPAR-γ, which are most typical and closely related to genes in bone regeneration, were detected by RT-PCR to explore whether PBMSCs took effect by impacting the expression of these cytokines. We also tried to find some valuable clues for the mechanism. Previous research revealed that PPAR-γ mainly exists in adipose tissues.[34] As some bone marrow is rich in fat, PPAR-γ proteins can also be detected.[35] Other studies have reported that PPAR-γ can promote bone marrow stromal cells to differentiate into adipose cells. When the PPAR-γ gene is activated, it can result in the accumulation of adipose cells and the pimelosis of medullary cavity.[34] In this research, the mRNA expression of PPAR-γ in the model FH generally increased, and that in the PBMSCT group was obviously lower than that in the CD group, in which there were more empty lacunae of osteocytes. This result was in line with that of histopathological morphology. BMP-2 mainly exists in the bone matrix and is closely related to bone regeneration. In addition, BMP-2 can induce undifferentiated bone marrow stromal cells to differentiate into osteoblasts. As a result, it can effectively boost bone repair and reconstruction.[36] The fact that the mRNA expression of BMP-2 was higher than the corresponding CD group at 8 weeks suggested that BMP-2 did do function in the repair of bone injury after PBMSCT. This result is consistent with that of radiographs and histopathological morphology in which more new trabecular bones were observed. The result also indicated that the treatment effect by PBMSCT, which was related to a decline of PPAR-γ expression and a rise of BMP-2 expression, is superior to that by the simplex CD.

In summary, this paper shows that rPBMSCs is successfully enriched and that the effect of rPBMSCs transplantation is superior than simple core decompression; affirms the effect of rPBMSCs therapy for ONFH; and preliminarily explores a relative mechanism. More detailed investigation of the mechanism is needed. Moreover, exploration of the amount and way of transplanted cells is essential, and it may provide evidence for its use in therapy of joint diseases by PBMSCs transplantation.

ACKNOWLEDGEMENTS

The authors would like to thank Dr. Chao Xie from the University of Rochester Medical Center for editing and submission consultation. This work was supported by grants from the National Natural Science Foundation of China (No.81060148).

REFERENCES

1. Smith DW. Is avascular necrosis of the femoral head the result of

http://dx.doi.org/10.3349/ymj.2016.57.4.1006

inhibition of angiogenesis? Med Hypotheses 1997;49:497-500.
2. Kang JS, Moon KH, Kim BS, Kwon DG, Shin SH, Shin BK, et al. Clinical results of auto-iliac cancellous bone grafts combined with implantation of autologous bone marrow cells for osteonecrosis of the femoral head: a minimum 5-year follow-up. Yonsei Med J 2013;54:510-5.
3. Bakhshi H, Rasouli MR, Parvizi J. Can local Erythropoietin administration enhance bone regeneration in osteonecrosis of femoral head? Med Hypotheses 2012;79:154-6.
4. Sun W, Li Z, Gao F, Shi Z, Zhang Q, Guo W. Recombinant human bone morphogenetic protein-2 in debridement and impacted bone graft for the treatment of femoral head osteonecrosis. PLoS One 2014;9:e100424.
5. Gemma G, Khan M, Haddad FS. Why do total hip replacements fail? Orthop Trauma 2015;29:79-85.
6. Avisar E, Elvey MH, Bar-Ziv Y, Tamir E, Agar G. Severe vascular complications and intervention following elective total hip and knee replacement: a 16-year retrospective analysis. J Orthop 2015;12:151-5.
7. Miric A, Inacio MC, Kelly MP, Namba RS. Are nonagenarians too old for total hip arthroplasty? An evaluation of morbidity and mortality within a total joint replacement registry. J Arthroplasty 2015;30:1324-7.
8. Ekmekci Y, Keven K, Akar N, Egin Y, Sengul S, Kutlay S, et al. Thrombophilia and avascular necrosis of femoral head in kidney allograft recipients. Nephrol Dial Transplant 2006;21:3555-8.
9. Bouamar R, Koper JW, van Rossum EF, Weimar W, van Gelder T. Polymorphisms of the glucocorticoid receptor and avascular necrosis of the femoral heads after treatment with corticosteroids. NDT Plus 2009;2:384-6.
10. Fraser JK, Wulur I, Alfonso Z, Hedrick MH. Fat tissue: an underappreciated source of stem cells for biotechnology. Trends Biotechnol 2006;24:150-4.
11. Fukuda S, Hagiwara S, Fukuda S, Yakabe R, Suzuki H, Yabe SG, et al. Safety assessment of bone marrow derived MSC grown in platelet-rich plasma. Regen Ther 2015;1:72-9.
12. Jones KB, Seshadri T, Krantz R, Keating A, Ferguson PC. Cell-based therapies for osteonecrosis of the femoral head. Biol Blood Marrow Transplant 2008;14:1081-7.
13. Beane OS, Fonseca VC, Cooper LL, Koren G, Darling EM. Impact of aging on the regenerative properties of bone marrow-, muscle-, and adipose-derived mesenchymal stem/stromal cells. PLoS One 2014;9:e115963.
14. Pak J, Lee JH, Jeon JH, Lee SH. Complete resolution of avascular necrosis of the human femoral head treated with adipose tissue-derived stem cells and platelet-rich plasma. J Int Med Res 2014;42:1353-62.
15. Pak J. Autologous adipose tissue-derived stem cells induce persistent bone-like tissue in osteonecrotic femoral heads. Pain Physician 2012;15:75-85.
16. Liu XH, Zhang T, Fang N, Zhang Q, Huang Y, Liu JW, et al. [Verification of multipotential mesenchymal stem cell presence in peripheral blood of rabbits]. Zhongguo Shi Yan Xue Ye Xue Za Zhi 2013;21:193-7.
17. Krstić J, Obradović H, Jauković A, Okić-Đorđević I, Trivanović D, Kukolj T, et al. Urokinase type plasminogen activator mediates Interleukin-17-induced peripheral blood mesenchymal stem cell motility and transendothelial migration. Biochim Biophys Acta 2015;1853:431-44.
18. Zhou Y, Singh AK, Hoyt RF Jr, Wang S, Yu Z, Hunt T, et al. Regulatory T cells enhance mesenchymal stem cell survival and proliferation following autologous cotransplantation in ischemic myocardium. J Thorac Cardiovasc Surg 2014;148:1131-7.
19. Liu XH, Zhang T, Zhang Q, Liu JW, Liu ZL, Tang NN. Colony forming capacity and neuron differentiation of rabbit peripheral blood-derived mesenchymal stem cells after G-CSF mobilization. J Xi'an Jiaotong Univ (Med Sci) 2014;35:26-9.
20. Zhou ZL, Zhang Q, Peng JC, Huang Y, Tang NN, Zhang T. Novel liquid nitrogen freezing method for establishing a rabbit model of femoral head osteonecrosis and its reliability evaluation. Acta Anatomica Sinica 2012;43:284-8.
21. Schmittgen TD, Livak KJ. Analyzing real-time PCR data by the comparative C(T) method. Nat Protoc 2008;3:1101-8.
22. Zvaifler NJ, Marinova-Mutafchieva L, Adams G, Edwards CJ, Moss J, Burger JA, et al. Mesenchymal precursor cells in the blood of normal individuals. Arthritis Res 2000;2:477-88.
23. Wan C, He Q, Li G. Allogenic peripheral blood derived mesenchymal stem cells (MSCs) enhance bone regeneration in rabbit ulna critical-sized bone defect model. J Orthop Res 2006;24:610-8.
24. Morikawa S, Mabuchi Y, Kubota Y, Nagai Y, Niibe K, Hiratsu E, et al. Prospective identification, isolation, and systemic transplantation of multipotent mesenchymal stem cells in murine bone marrow. J Exp Med 2009;206:2483-96.
25. Jones E, McGonagle D. Human bone marrow mesenchymal stem cells in vivo. Rheumatology (Oxford) 2008;47:126-31.
26. Wen Q, Ma L, Chen YP, Yang L, Luo W, Wang XN. A rabbit model of hormone-induced early avascular necrosis of the femoral head. Biomed Environ Sci 2008;21:398-403.
27. Yang C, Yang SH, Du JY, Li J, Xu WH, Xiong YF. Basic fibroblast growth factor gene transfection to enhance the repair of avascular necrosis of the femoral head. Chin Med Sci J 2004;19:111-5.
28. Wen Q, Ma L, Chen YP, Yang L, Luo W, Wang XN. A rabbit model of hormone-induced early avascular necrosis of the femoral head. Biomed Environ Sci 2008;21:398-403.
29. Hernigou P, Flouzat-Lachaniette CH, Delambre J, Poignard A, Allain J, Chevallier N, et al. Osteonecrosis repair with bone marrow cell therapies: state of the clinical art. Bone 2015;70:102-9.
30. Aoyama T, Fujita Y, Madoba K, Nankaku M, Yamada M, Tomita M, et al. Rehabilitation program after mesenchymal stromal cell transplantation augmented by vascularized bone grafts for idiopathic osteonecrosis of the femoral head: a preliminary study. Arch Phys Med Rehabil 2015;96:532-9.
31. Calori GM, Mazza E, Colombo M, Mazzola S, Mineo GV, Giannoudis PV. Treatment of AVN using the induction chamber technique and a biological-based approach: indications and clinical results. Injury 2014;45:369-73.
32. Peric M, Dumic-Cule I, Grcevic D, Matijasic M, Verbanac D, Paul R, et al. The rational use of animal models in the evaluation of novel bone regenerative therapies. Bone 2015;70:73-86.
33. Rosset P, Deschaseaux F, Layrolle P. Cell therapy for bone repair. Orthop Traumatol Surg Res 2014;100(1 Suppl):S107-12.
34. Shi XM, Blair HC, Yang X, McDonald JM, Cao X. Tandem repeat of C/EBP binding sites mediates PPARgamma2 gene transcription in glucocorticoid-induced adipocyte differentiation. J Cell Biochem 2000;76:518-27.
35. Gimble JM, Robinson CE, Wu X, Kelly KA, Rodriguez BR, Kliewer SA, et al. Peroxisome proliferator-activated receptor-gamma activation by thiazolidinediones induces adipogenesis in bone marrow stromal cells. Mol Pharmacol 1996;50:1087-94.
36. Wozney JM, Rosen V. Bone morphogenetic protein and bone morphogenetic protein gene family in bone formation and repair. Clin Orthop Relat Res 1998;(346):26-37.